Temporal cortex activation during speech recognition: an optical topography study

Hiroki Sato[a], Tatsuya Takeuchi[a], Kuniyoshi L. Sakai[a,b,*]

[a]*Department of Cognitive and Behavioral Science, Graduate School of Arts and Sciences, The University of Tokyo, Komaba, Tokyo 153-8902, Japan*
[b]*CREST, Japan Science and Technology Corporation (JST), Tokyo, Japan*

Abstract

Cortical activity during speech recognition was examined using optical topography (OT), a recently developed non-invasive technique. To assess relative changes in hemoglobin oxygenation, local changes in near-infrared light absorption were measured simultaneously from 44 points in both hemispheres. A dichotic listening paradigm was used in this experiment, in which target stimuli and non-target stimuli were presented to different ears. Subjects were asked to track targets and to press a button when targets shifted from one ear to the other. We compared three tasks: (i) a control task, in which a tone was used as the target; (ii) a repeat task, in which the target was one repeated sentence; (iii) a story task, in which the targets were continuous sentences of a story. The activity for the story task, compared with the repeat task, was localized in the left superior temporal cortex. Relative to the control task, we observed in this region a larger increase in oxyhemoglobin concentration and a decrease in deoxyhemoglobin concentration in the story task than those in the repeat task. These results suggest that the activity in the left temporal association area reflects the load of auditory, memory, and language information processing. © 1999 Elsevier Science B.V. All rights reserved.

Keywords: Speech recognition; Temporal association area; Hemoglobin oxygenation

1. Introduction

Optical topography (OT) is a recently developed non-invasive technique of functional mapping, which measures temporal changes in hemoglobin oxygenation simultaneously from multiple regions (Koizumi et al., 1999; Maki et al., 1995;

* Corresponding author. Tel.: +81-3-5454-6261; fax: +81-3-5454-6261.
E-mail address: sakai@mind.c.u-tokyo.ac.jp (K.L. Sakai)

Yamashita, Maki & Koizumi, 1996; Yamashita, Maki & Koizumi, 1999). OT is a new extension of near-infrared spectroscopy (NIRS) used to acquire a topographical image, whereas NIRS measures spectroscopic reflection and scattering from a single region with a light emitter and a detector (Chance, Zhuang, Unah, Alter & Lipton, 1993; Hoshi & Tamura, 1993; Kato, Kamei, Takashima & Ozaki, 1993; Villringer, Planck, Hock, Schleinkofer & Dirnagl, 1993). The technological development from NIRS to OT is conceptually similar to that from nuclear magnetic resonance (NMR) spectroscopy to magnetic resonance imaging (MRI). Measurement from multiple regions is achieved by independently modulating the intensities of each radiated laser beam, that is, by frequency encoding of spatial information (Yamashita, Maki & Koizumi, 1999). The minimum distance between measurement points of the current OT system is 21 mm, and minimum sampling interval is 100 ms.

There are several advantages of using OT over other functional mapping techniques. First, it is possible to independently measure the temporal changes in the concentrations of oxyhemoglobin and deoxyhemoglobin. Secondly, there is no scanning noise interfering with any auditory stimuli. Thirdly, its signal-to-noise ratio is relatively high, allowing for the observation of cortical activity even with a single trial. Finally, OT does not require a head constraint; thus its safe application to infants may make developmental mapping studies possible. One major disadvantage of OT is that its measurement is restricted to the cortical surface. Nevertheless, OT has a potential to open a new dimension for mapping human cognitive functions. Here we report the first successful application of this technique to the study of cortical responses during speech recognition. We have devised a dichotic listening task that requires intensive tracking of speech sounds and have compared a task with successive sentences of a story and that with repeated sentences. A portion of this study has been reported in abstract form (Sakai, Sato & Takeuchi, 1999).

2. Methods

2.1. Subjects

Seven male native Japanese speakers (ages: 21–32 years) participated in the present study. They showed right-handedness (laterality quotients: 81–100) by the Edinburgh inventory (Oldfield, 1971). The subjects' consent was obtained according to the declaration of Helsinki. Approval for the human experiments was obtained from the institutional review board of the University of Tokyo, Graduate School of Arts and Sciences.

2.2. Auditory stimuli

The auditory stimuli used in this study were speech sounds and non-speech sounds that were presented in speech-recognition tasks and a control task, respectively. All speech sounds were digitized (16 bit, 11 025 Hz) using speech synthesis software (Oshaberi-mate, Fujitsu, Tokyo, Japan) that converts Japanese written text into sound waveforms. Sine-wave tone and white noise used in the control task were

synthesized by sound-editing software (Sound Forge XP, Sonic Foundry Inc.). Speech sounds and non-speech sounds were presented with a stereophonic headphone at the peak of 60- and 58-dB sound pressure levels, respectively.

2.3. Task paradigm

A dichotic listening paradigm was used for all tasks in this study. Target stimuli and non-target stimuli were simultaneously presented to different ears every 2 s, and a target was alternatively presented to either the left ear or the right ear at random intervals. The frequency of presentation of targets was balanced between the left and right ears. Subjects were asked to track targets and to press a button when a target was shifted to the other side.

In the control task, a tone (sine wave: 1000 Hz) and white noise (low-pass cut-off frequency: 1000 or 10 000 Hz) were presented as targets and non-targets, respectively (duration: 1000 ms). In order to confirm that subjects performed tasks by recognizing targets, a tone of different pitch (sine wave: 300 Hz) was presented as a non-target at a lower rate. These probe stimuli prevented subjects from performing the tasks by tracking non-targets only.

We used two speech-recognition tasks: (1) a repeat task, in which the targets consisted of one repeated sentence, and (2) a story task, in which the targets were successive different sentences of a continuous story. In the repeat task, one sentence (duration: 1000–1530 ms, mean: 1270 ms) was repeated for a 36-s period, and different sentences were used in each period. Successive sentences for the story task were divided into phrases at natural break-points (duration: 590–1650 ms, mean: 1150 ms) for the presentation. In both tasks, a non-target was obtained by scrambling the sequence of syllables of the correspondent target. These jumbled stimuli conformed to the rules of Japanese phonotactics but had no meaning. A sentence different from the target for the repeat task and contextually anomalous phrases for the story task were used as probe stimuli. These tasks, therefore, cannot be completed appropriately by identifying speech sounds without paying attention to their meanings.

2.4. Experimental procedures

During the experiments, the subject sat in a chair with his eyes closed in a dark room. A pair of head shells with probe sockets was attached on both sides of the subject's head. In a single run with the repeat tasks (R), a 36-s period for the control task and the repeat task alternated three times, with one more control period at the end of a run. A single run with the story tasks (S) had the same alternation. Twelve runs were performed in the order of alternating S-R-R-S and R-S-S-R in one imaging session. Each subject was tested in at least two sessions. The first run of either S or R was counterbalanced by subsequent sessions.

After the experiment, a three-dimensional (3D) magnetic resonance (MR) image was taken of the subject to reconstruct a cortical surface image. Alfacalcidol beads (0.25 μg) buried in a head shell were used as MR markers, which can be identified on the MR image as spheres (diameter: 3 mm).

2.5. Optical topography procedures

We used two OT systems with the same calibration (ETG-100 and ETG-A1; Hitachi Medical Corporation, Tokyo, Japan), one for each hemisphere. Near-infrared laser diodes with two wavelengths (ranges: 782–793 and 823–832 nm) were used as the light sources (maximum intensity: 2 mW/mm^2: intensity modulation: 1–10 kHz). The reflected lights were detected with avalanche photodiodes located 30 mm from an incident position. Using lock-in amplifiers, the detected signal was separated into individual light sources with each wavelength (Yamashita et al., 1999). The transmittance data ln $T(\lambda,t)$ for a wavelength (λ) at measurement time (t) were obtained for each run.

The position of each MR marker was a midpoint between an incident point and a detection point. Each measurement point was defined as an intersection of the cortical surface and a perpendicular line from a marker point (Maki et al., 1996). Twenty-two points in each hemisphere were simultaneously measured at minimum spatial intervals of 21 mm, and each point was sampled every 500 ms. The measured region in each hemisphere centered on the Sylvian fissure and covered an area of 6×12 cm^2 (Fig. 1a).
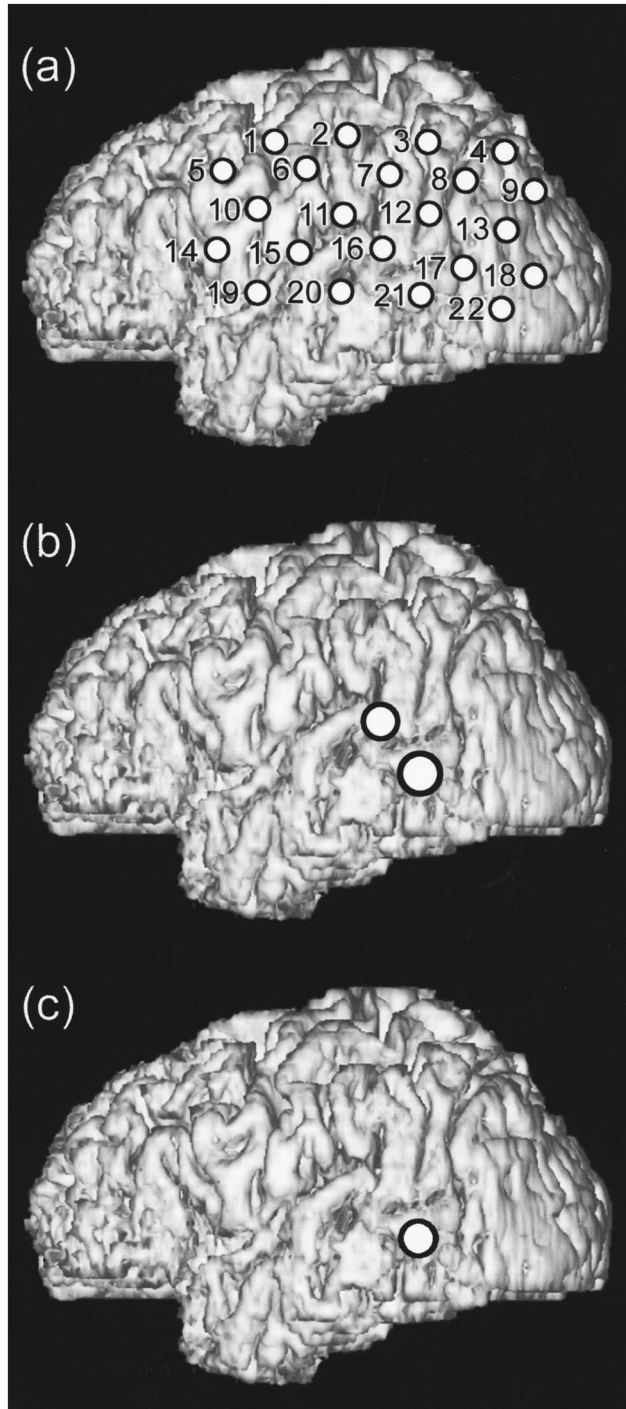
2.6. Data analyses

Time-series data of ln $T(\lambda,t)$ in a single run were baseline-corrected with a curve of the third degree, which was fitted for time points during the control task (Fig. 2). Either intrasubject data or intersubject data of multiple runs (R or S) were then averaged for each wavelength before calculating the relative hemoglobin changes. In the case of calculating the hemodynamics in the story run (S) relative to that in the repeat run (R), averaged runs under the two conditions were directly compared. We also compared R or S with the baseline curve in a similar manner. Because hemodynamic signals are relative changes from the baseline in the latter case, a long-range fitting, which spans more than one cycle of control-stimulation-control, should be used to estimate a baseline level throughout a single run (Fig. 2). By comparing ln $T(\lambda,t)$ under two conditions, the relative changes in oxyhemoglobin concentration (C_{oxy}) and deoxyhemoglobin concentration (C_{deoxy}) were calculated (Maki et al., 1995; Yamashita et al., 1996).

Relative hemodynamic changes were assumed to be delayed 6 s from the task periods in this study, and each shifted period of the story and repeat tasks was defined as an activation period. A correlation coefficient (r) of hemoglobin time points with a box-car waveform (each period: 36 s, delay: 6 s) was calculated for each measurement point (Bandettini, Jesmanowicz, Wong & Hyde, 1993; Watanabe et al., 1998), and we created an r-map from the r-values. As a threshold for the r-values, 0.73 or -0.73 was chosen for statistical significance ($P = 0.05$). This level of significance was determined from an equation

$$P = 2Q(TH \times N^{1/2})$$

where $Q(u)$ represents the upper probability of normal distribution above u, *TH* is a
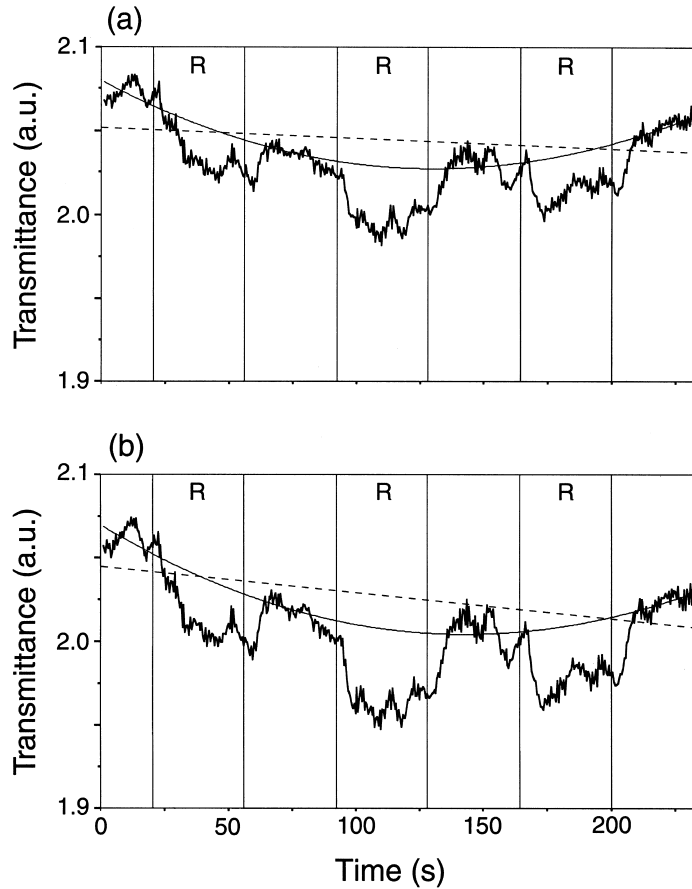
Fig. 2. Representative time courses of transmittance data at CH16 for one subject. (a) Data for a wavelength of 790 nm. (b) Data for a wavelength of 832 nm. Thick solid lines show the averaged transmittance data ln $T(\lambda,t)$ for each wavelength (λ) at time (t) in an arbitrary unit (a.u.). Note the prominent signal changes, which synchronize with each onset and end of three periods of the repeat task (R). For baseline correction, the data are fitted for time points during the control task with a curve of the third degree (thin solid lines). The relative difference between data for the two wavelengths is not affected when only linear interpolation is applied (broken lines), but we found that fitting with a third-degree curve was better than linear fitting for a long-range fitting, which resulted in a better signal-to-noise ratio.

Fig. 1. Superior temporal cortex activation in the story task. (a) The measurement points in the left hemisphere. The numbers represent channel numbers (CH) for the measurement points. The right hemi-sphere has the same arrangement of measurement points (CH 1 at the superior-anterior corner). Cortical surface images were reconstructed from 3D MR images of a representative subject. (b) The r-map of C_{oxy} in the story task relative to the repeat task. Circles at CH 16 ($r = 0.73$) and CH 21 ($r = 0.84$) are shown as activation points. The relative size of each circle represents the r-value. (c) The r-map of C_{deoxy} in the story task relative to the repeat task. Activation at CH 21 ($r = -0.73$) is shown. The r-maps for the right hemisphere are not shown here because there was no significant activation in this comparison ($r < 0.5$).

threshold of r, and N is the number of samples. N should be the number of independent samples, and here we assumed $N = 7$, which was the number of alternated periods in each run.

3. Results and discussion

3.1. Task performance

The behavioral accuracy and reaction times are shown in Table 1. Analysis of variance (ANOVA) indicated no main effect of tasks in the total performance $(F(2, 18) = 2.7, \ P > 0.05)$, or in the probe performance $(F(2, 18) = 3.3, \ P > 0.05)$. On the other hand, there was a main effect of tasks in the reaction time $(F(2, 18) = 7.5, P < 0.005)$. Post-hoc tests (Fisher's PLSD) revealed a difference between control and repeat tasks $(P < 0.05)$, and a difference between control and story tasks $(P < 0.005)$. The difference between repeat and story tasks, however, was not significant $(P > 0.1)$. These results suggest that the repeat and story tasks were equally balanced in terms of behavioral control for task difficulty.

3.2. Mapping the difference between the story and repeat tasks

The r-map for the hemodynamics in the story run relative to that in the repeat run shows a focal activation in the left superior temporal cortex (Fig. 1b,c). In these figures, r-maps for averaged data among subjects were superimposed on a representative cortical surface image of one subject. Two measurement points at channel 16 (CH 16) and channel 21 (CH 21) showed significant activation in C_{oxy} (Fig. 1b). These two measurement points were on the superior and middle temporal gyri. Comparing the individual mean hemoglobin changes during the story and repeat tasks (at a plateau level, from 10 s after the onset to the end of the task period) of CH 16 and those of CH 21, ANOVA (subjects × channels × periods) indicated the main effect of channels $(F(1, 32) = 4.2, P < 0.05)$ and no other main effects. The increase in C_{oxy} at CH 21 was significantly larger than that at CH 16. Moreover, the r-map in C_{deoxy} (Fig. 1c) showed CH 21 as a significant activation point. These

Table 1
Behavioral performance for tasks[a]

Task	Total accuracy (%)	Probe accuracy (%)	Reaction time (ms)
Control	97 ± 1.0	98 ± 0.8	660 ± 59
Repeat	97 ± 1.2	96 ± 1.3	870 ± 73
Story	93 ± 1.6	94 ± 1.1	990 ± 49

[a] Mean and standard errors are shown $(N = 7)$.

results showed that the activation in the story task relative to the repeat task was more prominent in the mid-lateral part (CH 21) of the left temporal cortex.

3.3. Spatial registration

We carefully assessed the measured areas among subjects using their 3D MR images. Based on Talairach coordinates (Talairach & Tournoux, 1988), the positions of measurement points were determined for each subject. The largest distance in the positions of the same measurement point among subjects was less than 18 mm in both hemispheres. The activated measurement points shown in Fig. 1b were confirmed to be on the superior and middle temporal gyri in all subjects (CH 16: $x = -65 \pm 2.0$, $y = -36 \pm 6.3$, $z = 16 \pm 5.0$; CH 21: $x = -64 \pm 1.9$, $y = -48 \pm 6.5$, $z = 5.9 \pm 5.5$).

3.4. Hemodynamic differences between the story and repeat runs

The hemodynamics in the story and repeat runs relative to the baseline were further examined. The temporal changes at CH 16 and CH 21 are shown in Fig. 3. With a delay of 6 s, an increase in C_{oxy} synchronized with each onset of the story task, and after reaching a plateau, C_{oxy} returned to the baseline level at the end of the task (Fig. 3a,b). Although a decrease in C_{deoxy} also synchronized with each period of the story task, C_{deoxy} did not exactly mirror the temporal dynamics of C_{oxy}. Similar, but smaller, changes in both C_{oxy} and C_{deoxy} were observed in the repeat run (Fig.
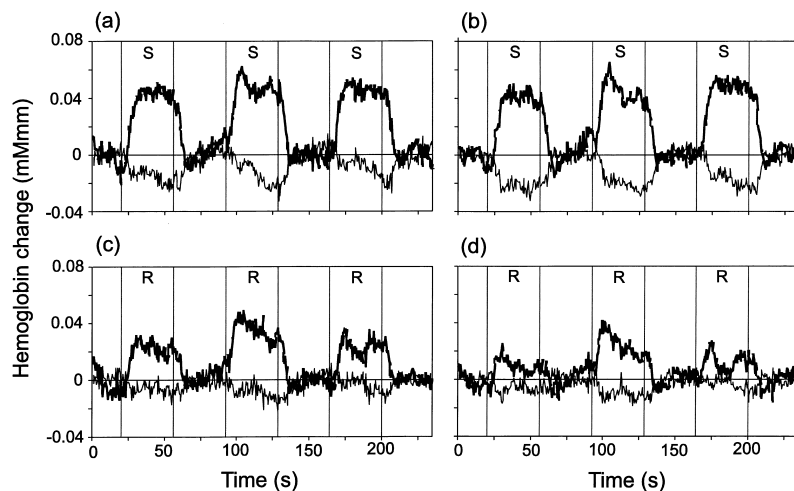

Fig. 3. Hemodynamics in speech-recognition tasks relative to the control task. (a) The story run at CH 16. (b) The story run at CH 21. (c) The repeat run at CH 16. (d) The repeat run at CH 21. Thick lines show the mostly positive temporal changes of C_{oxy}, whereas thin lines show the mostly negative temporal changes of C_{deoxy}. These temporal changes were calculated from averaged data among subjects. There are three periods of either the story task (S) or the repeat task (R) in each run.

3c,d). These results suggest that the hemodynamics reflects the processing of complex temporal and spectral features related to speech sounds.

These two measurement points (CH 16 and CH 21) showed similar hemodynamics, which was confirmed by significant temporal correlations ($P < 0.0001$) in the story task (C_{oxy}: 0.97, C_{deoxy}: 0.80) and in the repeat task (C_{oxy}: 0.88, C_{deoxy}: 0.65). Although CH 16 did not show significant activation for C_{deoxy} in the direct comparison (Fig. 1c), the hemodynamics at both measurement points were parallel when compared with the baseline.

After the two measurement points were averaged, the individual mean hemoglobin changes in the activation periods were statistically compared between the story and repeat runs (Fig. 4). Both the increase in C_{oxy} and decrease in C_{deoxy} during the story task were two times larger than those during the repeat task. ANOVA (subjects × tasks × periods) was performed separately for C_{oxy} and C_{deoxy}. This analysis indicated a significant main effect of tasks (C_{oxy}: $F(1, 12) = 36$, C_{deoxy}: $F(1, 12) = 36$, $P < 0.0001$) without any interactions.

3.5. Relationships between oxyhemoglobin and deoxyhemoglobin dynamics

We further examined two types of correlations between C_{oxy} and C_{deoxy} dynamics. Firstly, mean changes of either C_{oxy} or C_{deoxy} in each activation period were compared
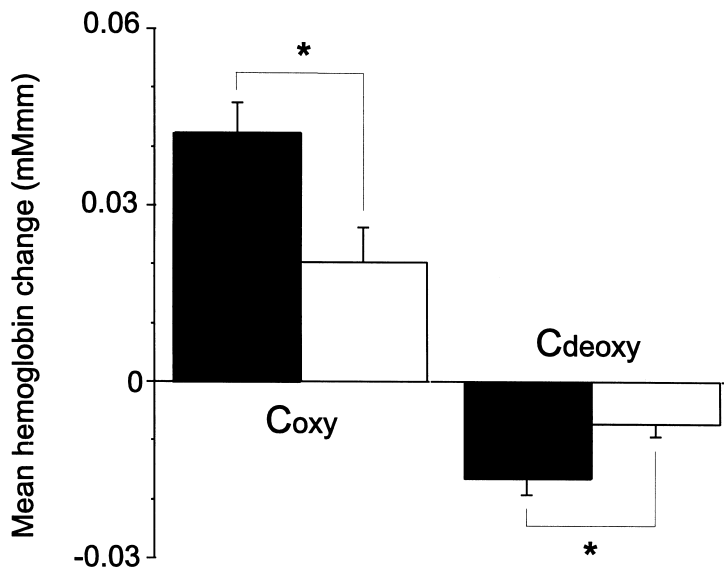

Fig. 4. Mean hemoglobin changes in the activation periods relative to the baseline. Each sample is intrasubject-averaged data of mean hemoglobin changes during each activation period, averaging CH 16 and CH 21. Error bars indicate the standard errors ($n = 21$). The filled bars denote mean hemoglobin changes in the story task, and the open bars denote changes in the repeat task. According to post-hoc tests (Fisher's PLSD), the differences between the story and repeat tasks were significant in both C_{oxy} and C_{deoxy} (*$P < 0.01$).

among subjects (CH 16 and CH 21 averaged). The intersubject correlation coefficient between mean C_{oxy} changes and mean C_{deoxy} changes was significantly negative in the story task (-0.71, $P = 0.0001$) and in the repeat task (-0.86, $P < 0.0001$). In both tasks, the more the mean C_{oxy} changes increased, the more the mean C_{deoxy} changes decreased. This result suggests that mean changes of both C_{oxy} and C_{deoxy} are useful indices of task activation that can be used for functional mapping.

Secondly, we compared each corresponding time point of C_{oxy} and C_{deoxy} in the activation periods of the story run for intersubject-averaged data. As indicated above, the exact temporal dynamics of C_{deoxy} did not mirror those of C_{oxy}. Accordingly, the temporal correlation coefficient between C_{oxy} and C_{deoxy} was not significant (0.11, $P > 0.1$, CH 16 and CH 21 averaged). These results indicate that the temporal changes of C_{oxy} and C_{deoxy} may reflect different physiological processes whose temporal dynamics are dependent over the long term (~30 s) but are different in the short term (<10 s).

3.6. Laterality

Hemispheric differences were examined by separately analyzing the temporal dynamics of C_{oxy} in the story and repeat runs. Channels (CH) for the measurement points with significant r-values are listed in Table 2. CH 16, 20, and 21 were located on the superior temporal cortex, and CH 15 and 19 were found on the Sylvian fissure in almost all hemispheres. Some of these measurement points showed activation in both hemispheres. It is clear that wider regions with more measurement points were activated in the story task than the repeat task in both hemispheres.

After the measurement points shown in Table 2 were averaged within each subject, the mean C_{oxy} changes in each activation period were examined among subjects. ANOVA (subjects × hemispheres × tasks × periods) indicated no main effect of hemispheres ($F(1, 44) = 0.10$, $P > 0.1$), but there was a significant interaction between hemispheres and tasks ($F(1, 44) = 5.5$, $P < 0.05$). Separate ANOVA for hemispheres indicated a main effect for tasks only in the left hemisphere (left, $F(1, 12) = 12$, $P < 0.01$; right, $F(1, 12) = 0.68$, $P > 0.1$). This result is consistent with the r-map of direct comparison between the story and repeat runs (Fig. 1).

Table 2
Comparison of measurement points with activation

Hemisphere	Task	Measurement points[a]
Left	Story	15, 16, 19, 20, 21
	Repeat	16, 20
Right	Story	15, 16, 19, 20
	Repeat	15, 19, 20

[a] Numbers shown are channels (CH) for the measurement points whose r-values were above the threshold of $r = 0.73$. These r-values were obtained by using C_{oxy} time courses, which were calculated from averaged data among subjects. These CH numbers correspond to positions in Fig. 1a.

4. General discussion

There are two major findings in the present OT studies. First, focal activation was found in the left superior temporal cortex, preferentially for the story task over the repeat task. Compared with the baseline, we confirmed that an increase in C_{oxy} changes and a decrease in C_{deoxy} changes synchronized with each period of the story run. Although similar changes were observed in the repeat run, the signal changes in the repeat run were half those in the story run. Secondly, we found a correspondence and dissociation between oxyhemoglobin and deoxyhemoglobin dynamics. The mean changes of C_{oxy} and C_{deoxy} in each activation period were negatively correlated, while the exact temporal dynamics of C_{oxy} and C_{deoxy} did not mirror each other.

There are some possible cognitive factors that are differentially involved in the story and repeat tasks. Repeating one sentence in the repeat task may cause a habituation of cortical responses. However, C_{deoxy} in the repeat task did not show an apparent decrease in signals after reaching the plateau level. A sustained habituation effect in the repeat task, if present, might result in a lack of C_{deoxy} change during the activation period, in contrast to C_{deoxy} in the story task (Fig. 3). But C_{oxy} in the repeat task showed signal changes parallel to those of C_{oxy} in the story task. Although we cannot exclude the involvement of transient habituation before reaching the plateau level, such a general repetition effect would have influenced many cortical regions, which was not the case in our observations.

Critical differences in cognitive factors between the story and repeat tasks would be the load of processing speech stimuli. Recognition of successive different sentences of a story demands more auditory, memory, and language information processing than the recognition of repeated sentences. The selective activation in the superior and middle temporal gyri reported here is consistent with the role of the primate temporal association area in memory storage and memory retrieval (Sakai & Miyashita, 1993). Further, our finding is consistent with a previous PET study that clearly showed an activation of the left superior and middle temporal gyri when subjects listened to continuous speech in their native language (Mazoyer et al., 1993). Moreover, the left middle temporal gyrus was activated only in that story condition among other conditions such as distorted stories, matching with the prominent activation of CH 21 in the present OT study.

From the current study, it is clear that the OT technique can be successfully applied to map the functional localization of cognitive factors, as well as to measure the temporal dynamics of cognitive activity. Because we found a correspondence and dissociation between oxyhemoglobin and deoxyhemoglobin dynamics, OT has the potential to provide novel information not previously obtained with other imaging techniques. Thus OT will open up new possibilities for studying cognitive function in the human cerebral cortex.

References

Bandettini, P. A., Jesmanowicz, A., Wong, E. C., & Hyde, J. S. (1993). Processing strategies for time-course data sets in functional MRI of the human brain. *Magnetic Resonance in Medicine*, *30*, 161–173.

Chance, B., Zhuang, Z., Unah, C., Alter, C., & Lipton, L. (1993). Cognition-activated low-frequency modulation of light absorption in human brain. *Proceedings of the National Academy of Sciences of the United States of America*, *90*, 3770–3774.

Hoshi, Y., & Tamura, M. (1993). Detection of dynamic changes in cerebral oxygenation coupled to neuronal function during mental work in man. *Neuroscience Letters*, *150*, 5–8.

Kato, T., Kamei, A., Takashima, S., & Ozaki, T. (1993). Human visual cortical function during photic stimulation monitoring by means of near-infrared spectroscopy. *Journal of Cerebral Blood Flow and Metabolism*, *13*, 516–520.

Koizumi, H., Yamashita, Y., Maki, A., Yamamoto, T., Ito, Y., Itagaki, H., & Kennan, R. (1999). Higher-order brain function analysis by trans-cranial dynamic NIRS imaging. *Journal of Biomedical Optics*, *4*, 403–413.

Maki, A., Yamashita, Y., Ito, Y., Watanabe, E., Mayanagi, Y., & Koizumi, H. (1995). Spatial and temporal analysis of human motor activity using non-invasive NIR topography. *Medical Physics*, *22*, 1997–2005.

Maki, A., Yamashita, Y., Ito, Y., Watanabe, E., & Koizumi, H. (1996). Spatial and temporal analysis of human motor activity using non-invasive optical topography. In R. R. Alfano, & J. G. Fujimoto, *OSA trends in optics and photonics on advances in optical imaging and photon migration*, (pp. 357–362). Washington, DC: Optical Society of America.

Mazoyer, B. M., Tzourio, N., Frak, V., Syrota, A., Murayama, N., Levrier, O., Salamon, G., Dehaene, S., Cohen, L., & Mehler, J. (1993). The cortical representation of speech. *Journal of Cognitive Neuroscience*, *5*, 467–479.

Oldfield, R. C. (1971). The assessment and analysis of handedness: the Edinburgh inventory. *Neuropsychologia*, *9*, 97–113.

Sakai, K., & Miyashita, Y. (1993). Memory and imagery in the temporal lobe. *Current Opinion in Neurobiology*, *3*, 166–170.

Sakai, K. L., Sato, H., & Takeuchi, T. (1999). Hemodynamic changes in auditory association cortex during speech recognition: functional mapping with optical topography. *Society for Neuroscience Abstracts 25, part 2, 1813*.

Talairach, J., & Tournoux, P. (1988). Co-planar stereotaxic atlas of the human brain. 3-dimensional proportional system: an approach to cerebral imaging. Thieme, Stuttgart.

Villringer, A., Planck, J., Hock, C., Schleinkofer, L., & Dirnagl, U. (1993). Near infrared spectroscopy (NIRS): a new tool to study hemodynamic changes during activation of brain function in human adults. *Neuroscience Letters*, *154*, 101–104.

Watanabe, E., Maki, A., Kawaguchi, F., Takashiro, K., Yamashita, Y., Koizumi, H., & Mayanagi, Y. (1998). Non-invasive assessment of language dominance with near-infrared spectroscopic mapping. *Neuroscience Letters*, *256*, 49–52.

Yamashita, Y., Maki, A., & Koizumi, H. (1996). Near-infrared topographic measurement system: imaging of absorbers localized in a scattering medium. *Review of Scientific Instruments*, *67*, 730–732.

Yamashita, Y., Maki, A., & Koizumi, H. (1999). A measurement system for non-invasive dynamic optical topography. *Journal of Biomedical Optics 4,* 414–417.